

Molecular Dynamics Study of Chemical Reactivity in Liquid Sulfur

Frank H. Stillinger* and Thomas A. Weber

AT&T Bell Laboratories, Murray Hill, New Jersey 07974 (Received: December 2, 1986)

Molecular dynamics simulation employing 1000 atoms has been used to examine rapid chemical reactions in fluid sulfur at high temperature. A combination of two-atom and three-atom potentials has been used to represent interactions, with specific forms chosen to improve our earlier exploratory modeling for sulfur. The rate of loss of S_8 rings from media initially composed entirely of these molecules has been measured at 870, 1050, and 1310 °C. Spontaneous formation of large linear polymers has been observed. Initial stages of the reaction sequences exhibit a peculiar dominance of species containing even numbers of atoms, which appears to stem from bond alternations produced by the model along diradical chains. The artificial system with only three-atom potentials operative is proposed as a suitable "reference substance" for implementing a perturbation theory of liquid sulfur at equilibrium, and molecular dynamics has been used to obtain the corresponding pair correlation functions both before and after quenching to potential energy minima.

I. Introduction

When the molecular dynamics simulation technique was first applied to the study of condensed matter, attention focused for practical reasons on models with pairwise additive central atomic interactions.^{1,2} Even so restricted, that early research activity produced important illuminating insights, particularly concerning the liquid states of the prototypical noble gases. Subsequent evolution of the computer and of computer simulation has permitted study of polyatomic and polar substances (such as carbon tetrachloride,³ water,⁴ and the alcohols.⁵) Pairwise additive

potential models however have largely remained the norm; in those few cases where nonadditive three-body interactions have been included they usually have influenced structure and other properties as relatively weak perturbations.^{6,7}

In order to model substances in which directed and saturable chemical bonds can form and break, pairwise additive potential functions are inappropriate. At a minimum, pair bonding in-

(1) Alder, B. J.; Wainwright, T. E. *J. Chem. Phys.* **1959**, *31*, 459.

(2) Rahman, A. *Phys. Rev.* **1964**, *136*, 405.

(3) McDonald, I. R.; Bounds, D. G.; Klein, M. L. *Mol. Phys.* **1982**, *45*, 521.

(4) Rahman, A.; Stillinger, F. H. *J. Chem. Phys.* **1971**, *55*, 3336.

(5) Jorgensen, W. L. *J. Am. Chem. Soc.* **1981**, *103*, 341, 345.

(6) Barker, J. A.; Bobetic, M. V. *J. Chem. Phys.* **1983**, *79*, 6306.

(7) Wojcik, M.; Clementi, E. *J. Chem. Phys.* **1986**, *84*, 5970.

teractions have to be supplemented by three-body terms of sufficient strength to cause qualitative changes in short-range liquid order, in low-temperature crystal structure, and in various transport and thermodynamic properties. A case in point is the tetrahedral semiconductor silicon, whose solid and liquid phases can at least be roughly simulated by using a classical Hamiltonian with two-atom and three-atom potentials.⁸ Another fascinating example is elemental sulfur, with many crystalline allotropes⁹ and various liquid and amorphous solid forms,¹⁰ all reflecting a chemical preference for divalency.

We have shown in an earlier paper¹¹ how a two-atom plus three-atom classical potential model can be selected to approximate the elaborate structural chemistry of sulfur, while retaining sufficient simplicity to make molecular dynamics simulation feasible for systems of respectable size ($N = 1000$). Our objectives in the present study have been, first, to improve the selection of interactions in the sulfur model to yield a more faithful description of the structural chemistry and, second, to use that improved model to study high-temperature chemical reactions by molecular dynamics simulation.

Section II presents the new sulfur potential, contrasts it with its predecessor, and indicates how the detailed changes were motivated. Stable structures for small gas-phase clusters have been determined for the new interaction, and these are also described in section II. The cyclic S_8 molecule is found to have special stability, in agreement with experiment but in contrast to our earlier and cruder model.

The stable low-temperature form of crystalline sulfur is orthorhombic and consists entirely of cyclic S_8 molecules arranged so that 16 inhabit a unit cell.⁹ The liquid just above the thermodynamic melting point (115.1 °C) consists predominately also of S_8 cyclic molecules.¹² Section III describes a molecular dynamics study of the low-temperature liquid, using the new interaction, in which the 1000 atoms utilized are aggregated into 125 S_8 cyclic molecules. In this low-temperature regime the potential barriers for bonding changes are so high that this molecular composition persists throughout any practicable molecular dynamics run. One must keep in mind that molecular dynamics simulations evolve in time about 10^{15} times more slowly than do the real systems they are designed to imitate, and chemical bond-breaking processes in liquid sulfur near its melting point have half-lives measured in hours.

This situation can be altered drastically by increasing the temperature. As demonstrated in our earlier paper,¹¹ S_8 ring-opening processes followed by a complex array of subsequent degradation and polymerization reactions can easily be observed during a molecular dynamics run. Section IV describes three molecular dynamics runs at elevated temperatures (870, 1050, and 1310 °C) selected to show the temperature dependence of cyclic S_8 chemical degradation. The tendency for the model to undergo spontaneous polymerization at high temperature is noted. Initial stages of the degradations are characterized by a peculiar persistence of sulfur molecules containing only even numbers of atoms; the "odd parity" molecules appear later than naive expectation might suggest.

Section V describes how the strongly degraded and highly reactive sulfur medium that appears at the end of the 1310 °C run of section IV, when quenched to considerably lower temperature, continues to undergo kinetic chemical processes. In particular, the mean molecular weight (on a per atom basis) rises dramatically as large linear polymers are formed.

One of the many attractive attributes of computer simulation is the ability to vary the interactions at will, to enhance qualitative

insights, and to suggest new lines of theoretical attack. In this spirit we have begun to investigate the model system which experiences only the three-body interactions of our present sulfur model. A few preliminary results for this hypothetical system have been summarized in section VI. Ultimately, this may be a suitable starting point into which the pair interactions could be continuously, reversibly, and isothermally coupled to attain the sulfur system of interest. Starting with the three-body part of the full sulfur interaction and then adding the conceptually simpler two-body part may at first glance seem to be the reverse of the natural choice. However, there is a compelling rationale for this ordering. The two-body potentials by themselves involve such strong bonding that their stable state at (and even well above) the melting temperature of sulfur is crystalline. Assuming that the primary interest lies in the fluid phases of sulfur, it is important that the unperturbed system likewise be fluid and that no phase transition be encountered during the reversible coupling process. The pure three-body system apparently fulfills this restriction.

Section VII provides a summary of results and presents several conclusions.

II. Atomic Interactions

We assume that atomic interactions in the condensed phases of sulfur can be represented by a single potential energy function of atomic positions $r_1 \dots r_N$, of the following type:

$$\Phi(r_1 \dots r_N) = \sum_{i < j = 1}^N v_2(r_{ij}) + \sum_{i < j < k = 1}^N v_3(r_i, r_j, r_k) \quad (2.1)$$

It is convenient to work in reduced units; the basic energy and length units are chosen to be

$$\epsilon = 100.797 \text{ kcal/mol}, \quad \sigma = 1.6836 \text{ \AA} \quad (2.2)$$

The pair potential in its correspondingly reduced form is

$$v_2(r) = 13.10937119(r^{-2} - 0.16)(r^{-2} - 0.25) \times \\ (r^{-2} - 1.07879) \exp[0.5/(r - 3.1)] \quad (r < 3.1) \\ = 0 \quad (r \geq 3.1) \quad (2.3)$$

This function has its absolute minimum at reduced distance 1.12246, with depth constructed to be -1.

Without loss of generality, the three-atom interaction v_3 has been taken to be a linear superposition of three terms that preserves interchange symmetry

$$v_3(r_1, r_2, r_3) = h(r_{12}, r_{13}, \theta_{213}) + h(r_{21}, r_{23}, \theta_{123}) + h(r_{31}, r_{32}, \theta_{132}) \quad (2.4)$$

where θ_{jik} stands for the angle at atom i subtended by atoms j and k . The reduced form of the function h is selected to be

$$h(r, s, \theta) = [75(\cos \theta - \cos 95^\circ)^2 + 25] \exp[3/(r - 2.5) + \\ 3/(s - 2.5)] \quad (r, s < 2.5) \\ = 0 \quad (\text{otherwise}) \quad (2.5)$$

Note that both v_2 and h are identically zero beyond respective cutoff distances of 3.1 and 2.5 but have been constructed so that all spatial derivatives are continuous across these singularities. Note also that v_3 is unchanged from its form in our earlier study.¹¹ The pair function v_2 however has been modified, in particular now to have a shorter cutoff (3.1 vs. 3.6). In both versions v_2 displays a low positive maximum beyond its absolute minimum and a shallow negative relative minimum at even larger distance. One motivation behind moving the cutoff inward was to reduce the apparently excessive intermolecular cohesive energy of the condensed phases.

The three-atom interactions v_3 are sufficiently large and positive to discourage more than two other sulfur atoms from clustering around, and simultaneously bonding by v_2 to, a third atom. Furthermore, the directionality inherent in v_3 (i.e., in h) is such that the angle between two pair bonds which can simultaneously be present will tend to occur at a chemically reasonable value (in the range 100–110°). The resulting preference for divalency with

(8) Stillinger, F. H.; Weber, T. A. *Phys. Rev. B: Condens. Matter* **1985**, *31*, 5262. Errata: *Phys. Rev. B: Condens. Matter* **1986**, *33*, 1451.

(9) Donohue, J. *The Structures of the Elements*; Robert E. Krieger Publishing: Malabar, FL, 1982; pp 324–369.

(10) Meyer, B., Ed. *Elemental Sulfur, Chemistry and Physics*; Wiley-Interscience: New York, 1965.

(11) Stillinger, F. H.; Weber, T. A.; La Violette, R. A. *J. Chem. Phys.* **1986**, *85*, 6460.

(12) Steudel, R. *Top. Curr. Chem.* **1982**, *102*, 149.

TABLE I: Reduced Values of the Potential Energy $\Phi_0(n)$ for Optimized Clusters of n Sulfur Atoms^a

n	$\Phi_0(n)$	$\Phi_0(n)/n$
2	-1.000 000 0	-0.500 000 0
3	-1.515 545 3	-0.505 181 8
4	-2.081 524 8	-0.520 381 2
5	-2.727 155 9	-0.545 431 2
6	-3.293 611 0	-0.548 935 2
7	-3.860 033 3	-0.551 433 3
8	-4.515 519 9	-0.564 440 0
9	-5.027 855 0	-0.558 650 6
10	-5.588 861 0	-0.558 886 1
11	-6.141 249 8	-0.558 295 4
12	-6.747 776 6	-0.562 314 7

^a We regard the searches as exhaustive only for $n < 9$.

controlled angles between successive bonds implies that small gas-phase clusters S_n ($n > 5$) will have nonplanar rings as their most stable forms.

At least among the relatively small cyclic S_n molecules (say $n < 50$), the cyclic octamer should exhibit the greatest stability. In other words, it should have the lowest negative value of $\Phi_0(n)/n$, the potential energy per atom in the cluster absolute-minimum geometry. In our earlier sulfur modeling study,¹¹ this quantity seemed to be at a minimum for $n = 10$, though it was very flat for $8 \leq n \leq 12$. A second motivation for modifying v_3 therefore has been to rectify this shortcoming.

Table I provides the new values of $\Phi_0(n)$ and $\Phi_0(n)/n$. While the latter still remains rather shallow as a function of n , the cyclic octamer is indeed the most stable on a per atom basis.

The most stable arrangement of three sulfur atoms is predicted to be an isosceles triangle, with apex angle 110.35° and reduced bond lengths 1.1663 (1.9636 Å). A higher lying local minimum, an equilateral arrangement with bond lengths 1.2028 (2.0250 Å), has also been observed for S_3 .

The tetramer S_4 also achieves its global potential minimum in an open structure, a nonplanar (and chiral) chain. The planar square structure is locally but not globally stable; evidently, ring closure in this case entails too much bond angle strain to be an absolute minimum.

Absolute minima whose energies appear in Table I for $n > 4$ all correspond to cyclic molecules. The pentamer S_5 is a planar symmetric structure. The larger cyclic clusters are nonplanar, with dihedral angles that tend to minimize occurrence of non-bonded pairs in the distance range at which v_2 has a relative maximum.

Many locally stable cluster arrangements have been uncovered for the larger n values represented in Table I. A particularly important subset of these are the open-chain structures ("diradicals"), with n sulfur atoms linked in linear sequence by $n - 1$ bonds. Typically, there will be several conformational options for these chains, each of which is a relative potential minimum. Regardless of conformation, the chains display an important structural feature (also evident in the earlier version¹¹): the shortest (and strongest) bonds are found at chain ends, and subsequent bonds moving toward the interior alternately are longer, shorter, ..., than average. These alternations damp out toward the interior of a long chain.

The cyclic S_8 molecule produced with the present interaction choice has bonds all of reduced length 1.2212 (2.0560 Å) and bond angles at each atom of 110.2° . In the orthorhombic crystalline phase of sulfur the corresponding average values⁹ are 2.06 Å and 108.0° , indicating reasonably good agreement considering that crystal forces may exert a slight perturbing influence.

The depth of the pair potential v_2 has been chosen to agree with the known energy of dissociating the dimer S_2 into neutral atoms.¹³ Energies of larger clusters involve intricate balances between v_2 and v_3 . Measurements of high-temperature sulfur vapor compositions have been used to infer enthalpies of the various S_n

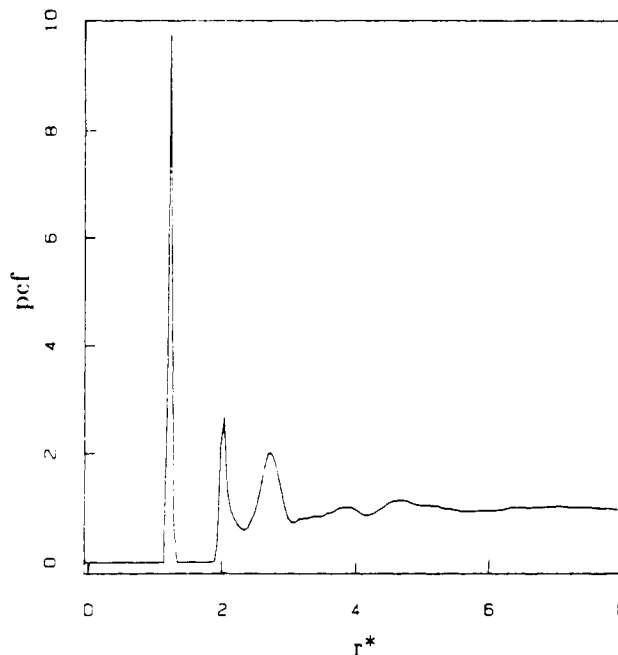


Figure 1. Atomic pair correlation function for liquid sulfur at 125.7 °C, consisting entirely of S_8 rings.

species,¹⁴ from which we conclude that $\Phi_0(n)/n$ should be about 0.011 reduced energy units (1.1 kcal/mol) lower for $n = 8$ than for $n = 6$. Table I shows that we predict this difference to be 0.0155 reduced energy units, perhaps indicating that further "fine tuning" of the potential energy form is warranted.

III. Low-Temperature Liquid Structure

The first molecular dynamics application of the revised interaction (eq 2.1–2.5) was determination of the local structure of the low-temperature liquid consisting entirely of S_8 rings. As before, we have employed $N = 1000$ atoms confined to a cubic unit cell with periodic boundary conditions. The length of the cubic cell edge was 18.3524 reduced units (30.90 Å), so that the corresponding mass density of sulfur, 1.805 g/cm³, agrees closely with that measured for the liquid near its melting point. The starting point was a liquid configuration generated in our earlier study,¹¹ with the 1000 atoms partitioned into 125 S_8 rings. Provided the temperature remains low, these molecules persist (compare section IV).

The measured melting temperature 115.1 °C corresponds to the reduced temperature

$$T_m^* = k_B T_m / \epsilon = 7.6576 \times 10^{-3} \quad (3.1)$$

Figure 1 shows the atomic pair correlation function $g(r)$ that has been calculated from a molecular dynamics run with mean reduced temperature 7.8663×10^{-3} (125.7 °C). This run began with the liquid well equilibrated at the prevailing temperature and spanned 1500 time steps Δt each of length 0.005τ , where

$$\tau = \sigma(m/\epsilon)^{1/2} = 4.6367 \times 10^{-14} \text{ s} \quad (3.2)$$

is the fundamental time unit.

The narrow peak shown by $g(r)$ in Figure 1 around reduced distance 1.25 comprises all covalently bonded pairs, which number precisely 1000 in this case. Numerically, no pairs whatever were found within the range of reduced distances

$$1.35 \leq r \leq 1.75 \quad (3.3)$$

so that identification of chemical bonds is unambiguous. Subsequent lower peaks centered around reduced distances 2.0 and 2.7 are dominated by nonbonded intramolecular pairs, but these lie upon a background of intermolecular pairs in the same range from neighboring S_8 rings. Qualitatively, these features were

(13) Huber, K. P.; Herzberg, G. *Molecular Spectra and Molecular Structure*; Van Nostrand Reinhold: New York, 1979; Vol. IV, p 564.

(14) Berkowitz, J.; Marquart, J. R. *J. Chem. Phys.* **1963**, *39*, 275.

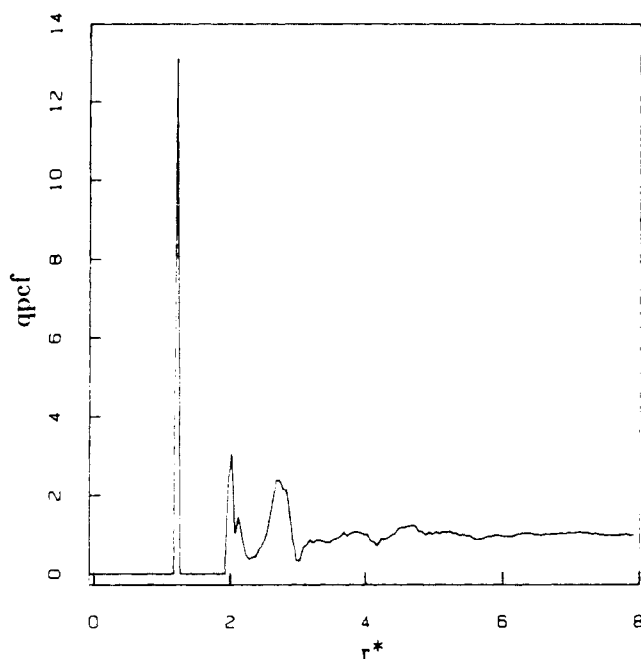


Figure 2. Quenched pair correlation function for a liquid consisting entirely of S_8 rings, initially at temperature 125.7°C .

observed in the earlier sulfur study as well, but detailed comparison shows there are substantial quantitative changes in short-range liquid order brought about by modification of the interactions.

As temperature rises, the clean separation between bonded and nonbonded pairs (as viewed from the perspective of the pair correlation function) begins to disappear. Strong vibrational amplitudes cause invasion of the vacant interval (eq 3.3) from both left and right. When chemical reactions are under way breaking and re-forming bonds, pairs move across this gap and begin to fill it up. The task of identifying bonds on an instant-by-instant basis then becomes ambiguous, and that in turn complicates the interpretation of molecular dynamics simulation designed to probe chemical reactivity.

We have adopted a convention which removes this difficulty. It requires that the instantaneous configuration be mapped by a steepest descent "quench" on its Φ hypersurface to the relevant local Φ minimum.¹¹ This quench procedure removes all vibrational distortion and by construction leaves the system in a mechanically stable state. We find that this mapping removes bonding ambiguity altogether, restoring the void in $g(r)$ between bonded and nonbonded pairs, regardless of how high the prequench temperature may have been. The procedure also has the benefit generally of sharpening the image of other aspects of short-range order in the liquid medium.¹⁵⁻¹⁷

Prior to applying these ideas to reactive high-temperature sulfur states, we observed the effect of steepest descent quenching on the low-temperature liquid of S_8 rings. Figure 2 displays a quench pair correlation function $g_q(r)$ from the same state for which Figure 1 provided the conventional $g(r)$. Specifically, this represents the distribution of pair distances in a *single* configuration, obtained by applying the steepest descent quench to the end point of the cited 1500-step run. That only a single potential energy minimum was located reflects the difficulty of locating such configurations with high precision in the given 3000-dimensional space. But in most important respects we find that the resulting $g_q(r)$ features are reproducible from one quench to the next, provided the same physical state supplied the initial conditions.

Comparison of Figures 1 and 2 shows that quenching has clearly enhanced the image of short-range order. In particular, the peak due to bonded pairs has narrowed and heightened (while still comprising exactly 1000 bonds). Furthermore, the subsequent

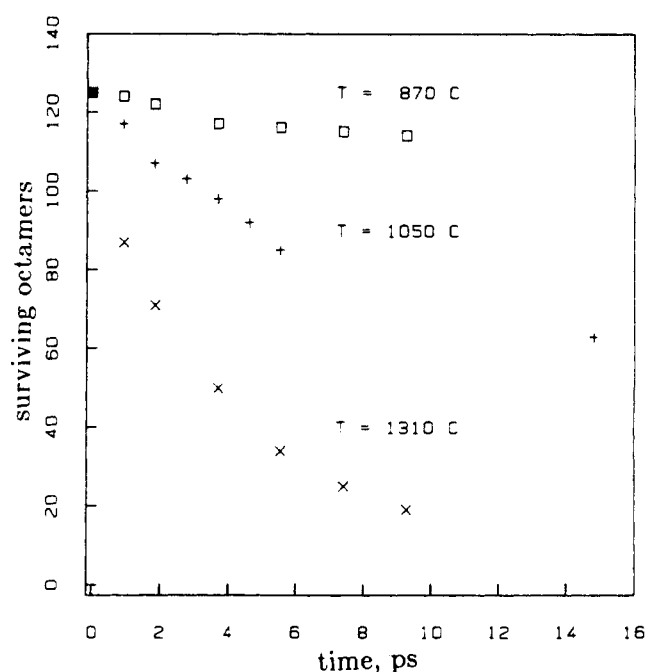


Figure 3. Time dependence of S_8 ring survival at three elevated temperatures. The density is held fixed at 1.805 g/cm^3 . The identification of molecular species at any instant is based upon the steepest descent mapping on the potential energy hyperspace, described in the text.

peak is now partially resolved into distinguishable components.

IV. Octamer Ring Degradation

The final configuration of the molecular dynamics run reported in section III served as the generator of high-temperature runs during which S_8 ring decomposition was monitored. For each of the three runs carried out, a suitable scalar factor was applied in common to all particle momenta of that final configuration, thereby instantaneously raising the system energy and temperature to the range desired. Chemical bonds were identified during the runs by the procedure just outlined. (After quenching, any $r_{ij} < 1.50$ was regarded as a bond.) Molecular species present in the system at any time are the atom clusters connected by bonds. These species were classified by the number of atoms they contained and whether topologically they were cyclic molecules, open chains, or other species. Hence, by carrying out repeated quenches to potential energy minima, it was possible to monitor the time-dependent survival of the initial species, the 125 S_8 rings.

Three high-temperature runs have been carried out. The mean temperatures during those runs were 0.0225, 0.0260, and 0.0313 in reduced units (respectively 870, 1050, and 1310°C), and the corresponding run lengths were 9.27, 14.84, and 9.27 ps.

Figure 3 shows the number of surviving S_8 rings as time progresses for each of the three runs. Quite obviously, the chemical decomposition processes (which were far too slow to observe by computer simulation near T_m) have been accelerated into the simulation time regime. Furthermore, the results in Figure 3 show considerable temperature dependence, as should be expected.

The survival data shown in Figure 3 can crudely be fitted to a single-exponential decay

$$N_{e8}(t) \cong 125 \exp[-t/t_0(T^*)] \quad (4.1)$$

where T^* stands for the reduced temperature $k_B T/\epsilon$. Assuming an "Arrhenius" temperature dependence for the degradation rate, we find

$$\ln [t_0(T^*)/\tau] \cong 0.29 T^{*-1} - 4.73 \quad (4.2)$$

where τ is the fundamental time unit given earlier in eq 3.2. It is quite uncertain whether extrapolation to the melting point is meaningful, but nevertheless, doing so formally indicates

$$t_0(T_m^*) \cong 11.5\text{ s} \quad (4.3)$$

Although this is still substantially shorter than the hours-long

(15) Stillinger, F. H.; Weber, T. A. *J. Chem. Phys.* **1984**, *80*, 4434.

(16) Stillinger, F. H.; Weber, T. A. *Science* **1984**, *225*, 983.

(17) Stillinger, F. H.; La Violette, R. A. *J. Chem. Phys.* **1985**, *83*, 6413.

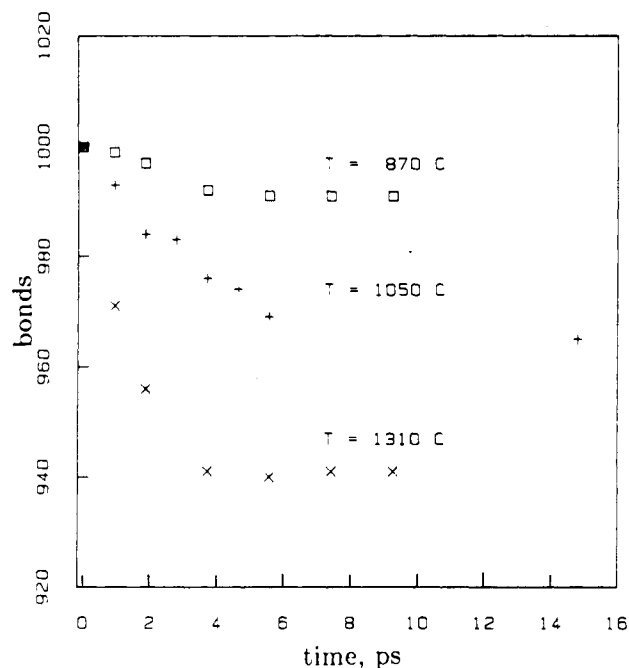


Figure 4. Time dependence of the number of covalent bonds in sulfur at elevated temperature. All three runs initially contained 125 cyclic S_8 molecules.

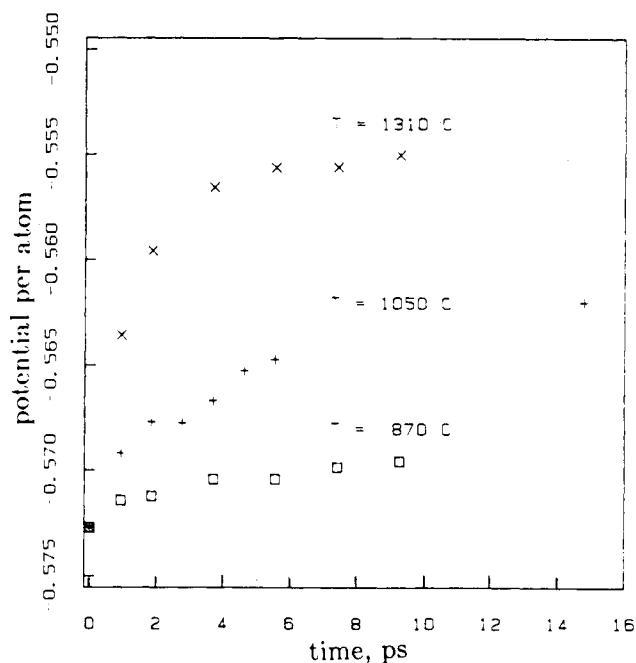


Figure 5. Depths of potential energy minima within whose multidimensional basins the high-temperature sulfur runs moved as the various chemical reactions proceeded.

lifetimes observed experimentally near T_m^* , it is not absurdly out of line.

The time dependence of the total number of covalent bonds is shown in Figure 4 for the three high-temperature runs. The initial decline from the 1000 bonds present in the 125 cyclic S_8 molecules is attributable to thermally induced ring opening to yield S_8 diradical chains. However, it is clear that the results in Figure 3 do not map simply into those of Figure 4. The 1310 °C run particularly shows a leveling of total bond number while the cyclic S_8 molecules are still being consumed rapidly. The same phenomenon also seems to be present in the 1050 °C run, though less vividly. This feature is attributable to the polymerization processes discussed below.

As our small-cluster calculations have illustrated, bond breakage is endothermic. Therefore, we would expect that the depths of

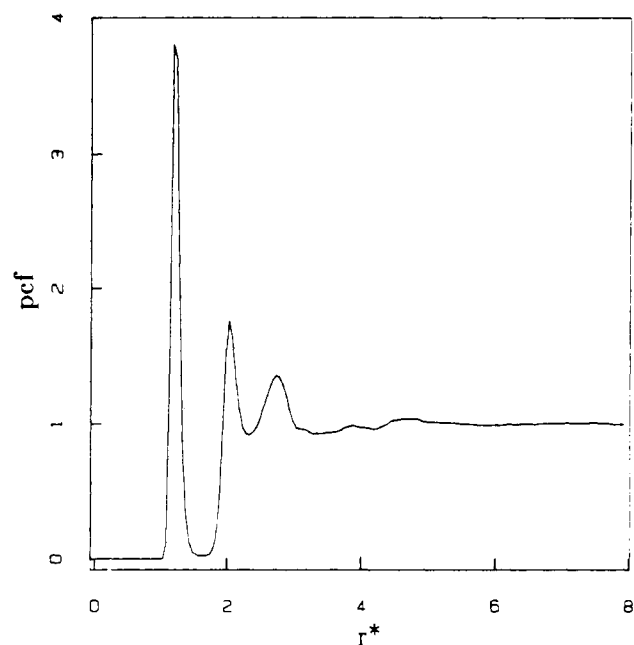


Figure 6. Conventional pair correlation function evaluated during the last 4000 steps (0.927 ps) of the 1310 °C reaction run.

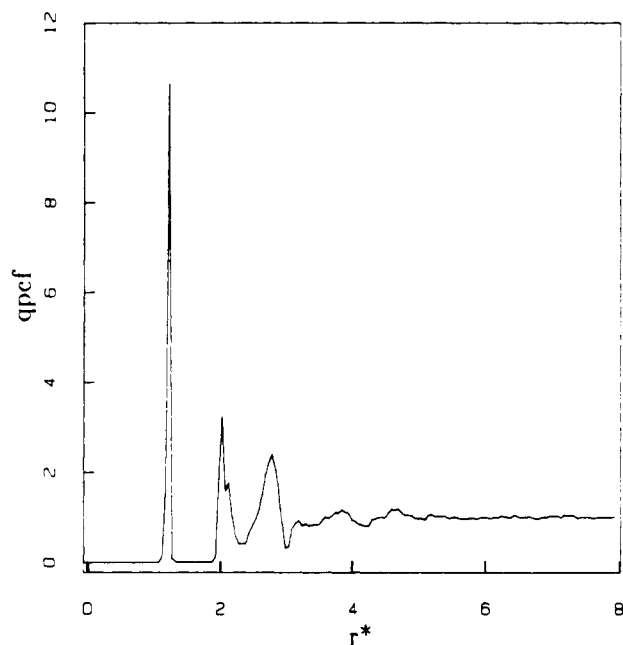


Figure 7. Quench pair correlation function for the final configuration of the 1310 °C reaction run.

potential energy minima visited by the 1000-atom system during the course of a high-temperature run would drift upward. And indeed drift should be faster the higher the temperature. Figure 5 presents the depths of the minima probed by our steepest descent mapping for the three runs, showing that expectations are confirmed.

Comparison of prequench and postquench pair correlation functions for these high-temperature reactive media stresses the basic importance of carrying out the mapping to minima in order to identify molecular species unambiguously. Figures 6 and 7 provide a comparison from the end of the 1310 °C run. The conventional pair correlation function $g(r)$ exhibited in Figure 6 is a time average over the last 4000 time steps (0.927 ps) of the run, while the vibration-free $g_q(r)$ shown in Figure 7 pertains only to the single quench configuration at the end of the run. Although $g(r)$ is small at its first minimum (≈ 0.022), it is not zero as is $g_q(r)$, and in fact this nonzero value is apparently composed of both bonded pairs that have vibrated strongly outward as well as nonbonded pairs that have vibrated strongly inward, the pro-

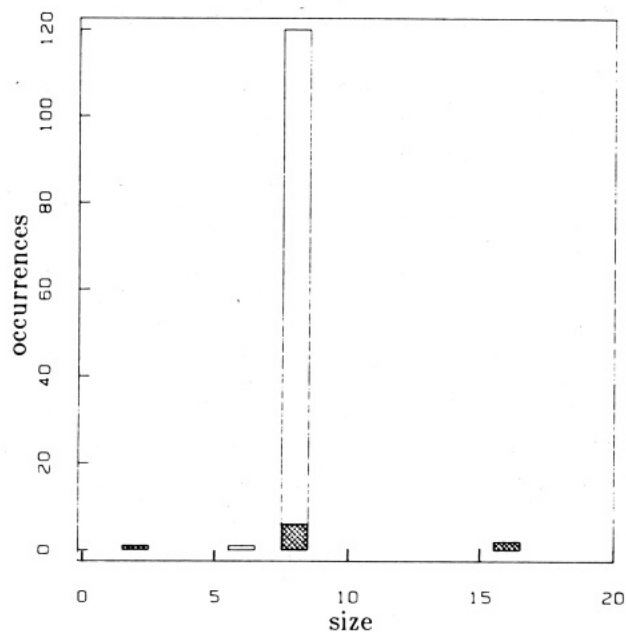


Figure 8. Molecular composition of the sulfur medium at the end of the 870 °C run. Rings and chains are indicated by white and by shading, respectively.

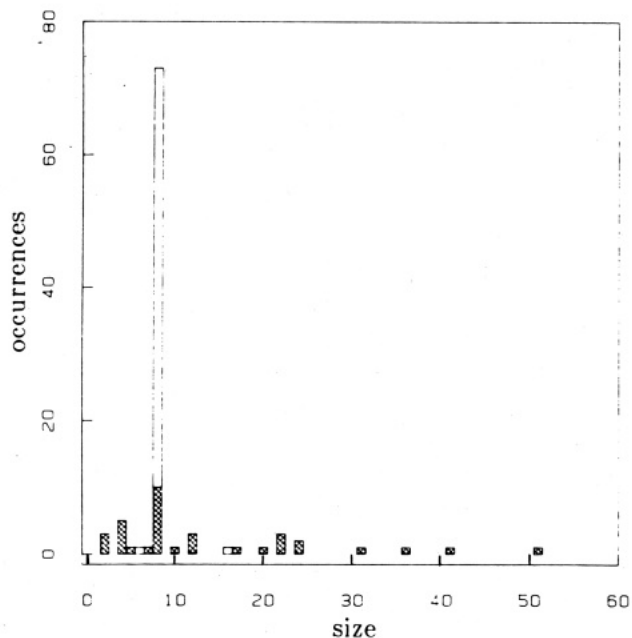


Figure 9. Molecular composition of the sulfur medium at the end of the 1050 °C run. Cyclic species are indicated by white, and diradical chain species by shading.

portions of which are unknowable from $g(r)$ alone.

By comparison of $g_q(r)$ for the unreacted low-temperature liquid (Figure 2) with that in Figure 7 after substantial reaction (as well as others we have plotted but do not reproduce here), it becomes clear that this quantity is sensitive to chemical reactions principally by the magnitude of its first peak, i.e., the number of chemical bonds present. Features in $g_q(r)$ at larger distances, such as the partially resolved second peak, show only subtle changes. While $g_q(r)$ clearly indicates and supports the algorithm that should be used to identify chemical bonds, it does not reveal the topologies by which these bonds connect atoms into clusters (molecules).

Figures 8–10 provide a complete topological accounting of the bonding patterns, or molecules, present at the end of each reaction run. Only cyclic molecules and open chains were encountered at the end points of the two lower temperature runs, and they are indicated as white and as shaded portions of the histograms. The highest temperature run end point exhibited branched species,

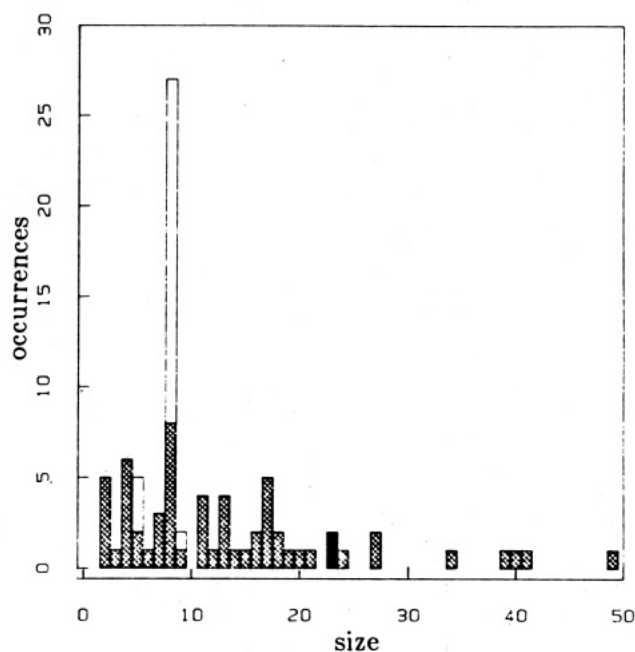


Figure 10. Molecular composition of the sulfur medium at the end of the 1310 °C run. Cyclic and chain species are indicated by white and by shading, respectively. Branched species are indicated by black.

discussed below and indicated in Figure 10 in black. These presentations make it clear that following the earliest reaction stage during which S_8 ring opening is the only reaction event, chain scission and polymerization reactions begin to take place. These parallel and coupled reaction pathways clearly can produce a broad distribution of molecular weights in the long-time limit.

The histogram in Figure 8 for reaction at 870 °C illustrates an unanticipated phenomenon. All molecules contain an even number of sulfur atoms, even while scission and polymerization processes have begun. This persistence of only even-numbered species is also seen throughout the first half of the 1050 °C run, after which cyclic and open S_n molecules with

$$n = 2, 4, 6, 8, 10, 12, 14, 16, 22, 24 \quad (4.4)$$

are observed. Subsequently, odd n values begin to appear. The same kind of sequence also arises at 1310 °C, but much compressed in time; after 4000 time steps (0.927 ps) have elapsed the only odd-numbered molecules found are single chains with $n = 9$ and 15 embedded in an otherwise “even” medium with n ranging from 2 to 16.

The key to the initial persistence of even numbers n appears to lie in the bond length and strength alternation noted in section II for open chains. Relatively weak bonds along an open chain are the second, fourth, ..., bonds from each end. These would be expected preferentially to cleave under high-temperature conditions, thereby splitting off S_2, S_4, \dots . If the starting chain contained an even number of atoms, so too will the resulting fragments. The first chains formed, by ring opening, are of course even. End-to-end linkage of even chains likewise preserves even parity. Although considerably slower, thermal cleavage of the stronger bonds along a chain (particularly in the middle of a long chain where successive bonds are barely distinguishable) eventually should and does occur to begin mixing odd species into the sulfur medium.

A few of the intermediate state quenches and the final state of the high-temperature run show unusual clusters that are neither chains nor rings but contain single trivalent sulfur atoms. These are branched “starfish” or “tadpole” structures consisting of a chain of variable length attached at one of its ends to an atom within another chain or ring, respectively. Such infrequent structures were also detected in our earlier sulfur simulations,¹¹ and the available evidence suggests they may be important as reaction intermediates in ring opening. In agreement with our model, *ab initio* quantum calculations¹⁸ indicate that neutral sulfur clusters

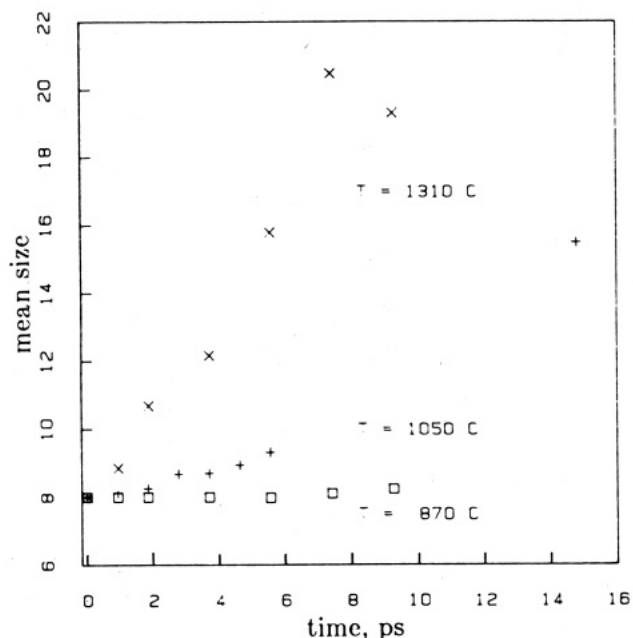


Figure 11. Time dependence of the mean molecular size d (defined in eq 4.6) for the high-temperature reaction runs.

with trivalent sulfur atoms can indeed have local stability, but they are never found in the lowest energy structures.

Let n_j stand for the number of clusters (molecules) containing exactly j sulfur atoms. The n_j vary during reaction, but the total number of atoms N is conserved:

$$N = \sum_{j=1}^N j n_j \quad (4.5)$$

The mean molecular size, or mean degree of polymerization, on a per atom basis is given by

$$d = N^{-1} \sum_{j=1}^N j^2 n_j \quad (4.6)$$

This quantity is exactly 8 at the start of our reaction runs and then drifts upward as the various reactions proceed. Figure 11 shows the d values computed from quenches during the runs. It is clear that entropic driving forces created by high temperature cause the medium to polymerize, in agreement with observations on the real material.¹⁰

V. Lower Temperature Polymerization

Evidence shown in Figures 3–5 and Figure 11 suggests that the 1310 °C run may be approaching a steady state at its final configuration. The species histogram in Figure 10 shows that the medium is very reactive at that stage, with a high concentration of diradical chains. We decided to gauge this reactivity by suddenly lowering the temperature and observing what subsequent species changes ensued.

Specifically, all atom momenta were set to zero at the end of the 1310 °C run, and then molecular dynamics at the conserved lower system energy was carried forth for 204000 time steps (47.29 ps). The average reduced temperature during this extension was 0.0198, i.e., 730 °C. The configuration at the end of this extension was mapped onto the relevant potential energy minimum as usual, by the steepest descent procedure, to permit unambiguous identification of the chemical species then present.

Figure 12 provides the final assay. In spite of the lowered temperature, the polymerization process has continued unabated, owing to the high concentration of reactive species. The largest molecules observed are S_{134} , S_{153} , and S_{157} diradical chains. The quantity d , which measures the mean molecular size, has risen from 19.306 at the beginning of this extension to 89.464 at the end. No tadpoles were detected in the final configuration.

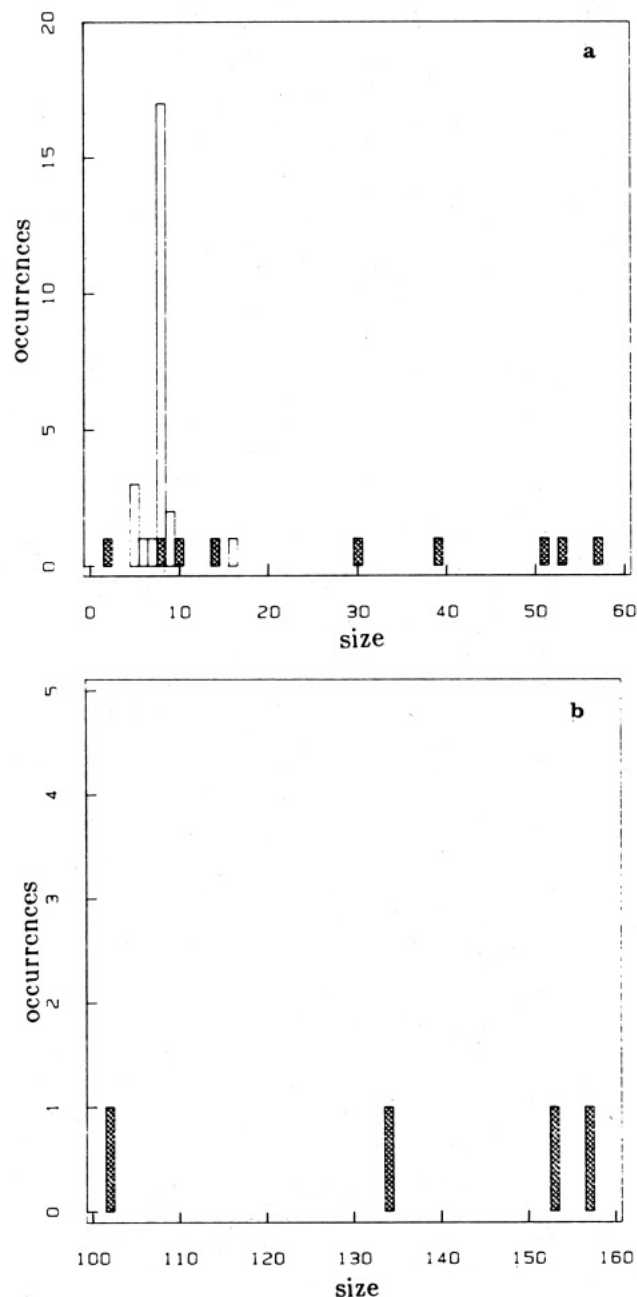


Figure 12. Molecular composition at the end of the 730 °C polymerization extension, which follows the 1310 °C reaction run. The distribution is presented in two parts, (a) and (b), for clarity.

The respective reduced values of the potential energy in the mapping minima at the beginning and at the end of the extension are -555.0049 and -565.4184 . This spontaneous downward drift primarily stems from the increase in number of covalent bonds, namely from 941 to 987. However, it represents only a bit more than half the lowering that would be required to return to those minima on the Φ hypersurface corresponding exclusively to intact S_8 rings.

Nineteen intact S_8 rings were present at the beginning of the extension run, all survivors of the preceding high-temperature treatment. On the basis of the S_8 ring destruction rates shown earlier in Figure 3, it seems reasonable to guess that at most just one of the 19 S_8 rings would disappear during the 730 °C extension run. In fact, only 16 S_8 rings were found at the end of this reduced-temperature extension. The explanation seems simply to be that the medium is more reactive on account of the high chain diradical concentration initially present, compared to the concentration expected if the medium were brought directly to 730 °C from low temperature. The behavior of the sulfur system exhibits a substantial chemical memory effect.

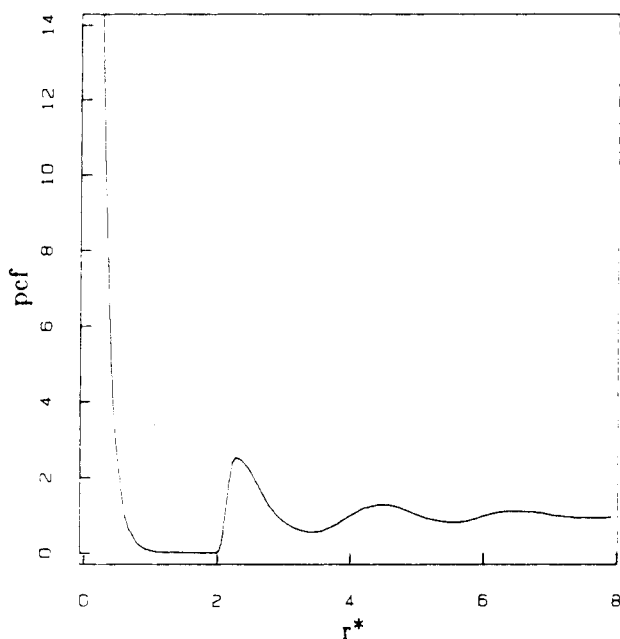


Figure 13. Conventional atomic pair correlation function $g(r, \lambda=0)$ for the model fluid in which only the three-body interactions v_3 operate. The reduced temperature is 0.008 01, corresponding to 133.0 °C.

VI. Three-Body Fluid

Our sulfur model is of necessity very complicated, compared for example to corresponding models for liquified noble gases in which only additive pair interactions are present. It could not be otherwise, considering the complexity of the structural chemistry, the crystallography, and the reaction kinetics that need to be represented. However, this amplifies the difficulties that must be faced when attempting to devise analytical theory as a supplement to brute-force simulation.

One option which seems to hold promise as a theoretical approach to understanding the sulfur model is perturbation theory. We have begun to consider a trivial generalization of the Φ expression, eq 2.1, where a continuously variable coupling constant λ multiplies the pair potential contributions:

$$\Phi(r_1 \dots r_N, \lambda) = \lambda \sum_{i < j=1}^N v_2(r_{ij}) + \sum_{i < j < k=1}^N v_3(r_i, r_j, r_k) \quad (6.1)$$

Setting $\lambda = 1$ recovers the previous case; setting $\lambda = 0$ yields an N -body system in which only the three-body interactions v_3 operate. We suggest that this latter situation offers a convenient reference fluid with rather simple properties and that attention can usefully be focused on the continuous perturbation produced by increasing λ from zero to unity. As mentioned in the introductory remarks, using the pair interactions alone as a reference system (then coupling in the v_3 part) is inappropriate for studying the fluid phases of sulfur, since the attractive well of v_2 is so deep and the melting temperature therefore so high.

Our coupling procedure represents a minor generalization of one introduced into liquid state theory many years ago by Kirkwood.^{19,20} By use of this approach, elementary principles of statistical mechanics suffice to derive an expression for $f(T, \rho)$, the Helmholtz free energy per particle, in the conventional large system limit:

$$f(T, \rho) = f_0(T, \rho) + \frac{1}{2} \rho \int_0^1 d\lambda \int dr v_2(r) g(r, \lambda) \quad (6.2)$$

Here $f_0(T, \rho)$ stands for the per particle Helmholtz free energy in the reference system, $g(r, \lambda)$ is the atomic pair correlation function in the partially coupled system, and the λ integral is to be carried out at constant temperature T and density ρ . Other thermodynamic quantities can be derived from f by standard identities.

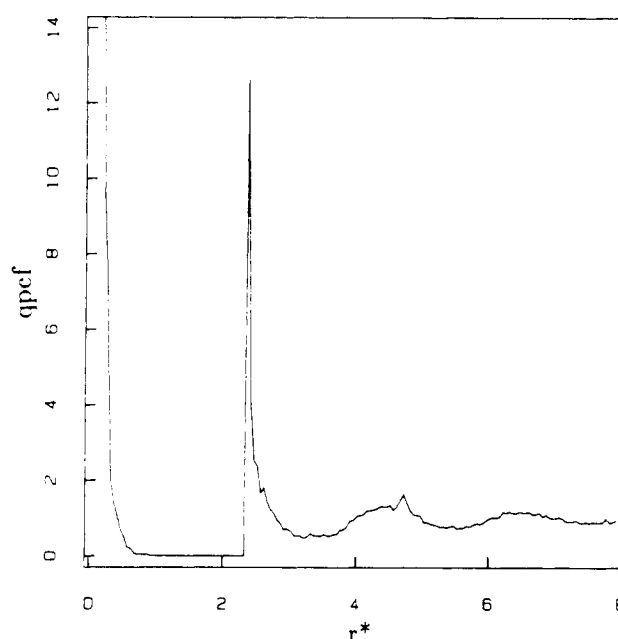


Figure 14. Quench pair correlation function $g_q(r, \lambda=0)$ generated by the final configuration of the molecular dynamics run on which Figure 13 was based.

Figure 1 presents a pair correlation function $g(r, 1)$ for the fully coupled case. (We assume that pure S_8 ring composition is close to the equilibrium composition at the temperature considered in Figure 1.) To understand the other extreme represented by the three-body reference fluid, we have also used molecular dynamics (same N and ρ as above) to examine $g(r, 0)$. With this simplified potential Δt could be increased to 0.01τ . Figure 13 shows the surprising result at reduced temperature 0.008 01 (133.0 °C), only slightly above the melting point for real sulfur. A very large peak near vanishing distance appears, demonstrating a tendency for atoms to form compact clusters. That $g(r, 0)$ essentially vanishes in the range of reduced distances $1 < r < 2$ means that these clusters are well separated from one another. Low peaks beyond reduced distance 2 reflect short-range spatial correlations between these clusters.

By applying the earlier "bonding" criterion (with cutoff distance 1.50), one discovers that the compact clusters are predominantly close pairs, with a few single atoms. Clusters of more than two atoms do not occur. At the end of the 2000-step (0.927 ps) run on which Figure 13 was based, there were 490 close pairs in the system and 20 isolated atoms.

The three-body system has discovered that arranging particles in close pairs, with those pairs well separated from one another, is an effective way to minimize the totality of the nonnegative three-body interactions. A third particle is almost always too far away from any two others to create a significant v_3 value.

The image of short-range order due to spatially separated compact pairs (plus a few unpaired atoms) can be enhanced by the mapping-to-minima steepest descent procedure invoked earlier. Figure 14 shows $g_q(r, 0)$ prepared from the final configuration of the run upon which Figure 13 was based. The small-distance peak for intrapair correlation has become enormously large ($\approx 6 \times 10^3$) and for practical purposes has been vertically truncated in Figure 14. The substantial sharpening of the second peak in $g_q(r, 0)$ with an inner discontinuity makes the intercluster correlations resemble somewhat the random packing of hard spheres.²¹⁻²³ After the steepest descent quench, the system contains 492 close pairs and 16 isolated atoms.

As λ begins to increase from zero, the divergent repelling core in v_2 will have the effect of forcing compact pairs apart. Continuation of this coupling process would subsequently encourage

(19) Kirkwood, J. G. *J. Chem. Phys.* **1935**, *3*, 300.
(20) Kirkwood, J. G. *Chem. Rev.* **1936**, *19*, 275.

(21) Finney, J. L. *Proc. R. Soc. London, A* **1970**, *319*, 479.
(22) Bennett, C. H. *J. Appl. Phys.* **1972**, *43*, 2727.
(23) Finney, J. L. *Nature (London)* **1977**, *266*, 309.

bonded pairs to link up in formation of chains and eventually rings as in the fully coupled model. It will be important to see whether manipulation of λ in series of molecular dynamics simulations at low temperature can hasten the otherwise very slow attainment of chemical equilibrium.

VII. Summary and Conclusions

Our first attempt¹¹ at modeling liquid sulfur demonstrated that at least the gross features of the structural chemistry of that element could be reproduced with a combination of two-atom and three-atom potentials. The present study reports a refinement in choice of those potentials which improves the fidelity of description and in particular gives cyclic S_8 molecules special stability. No doubt further refinements are still possible, but probably any serious effort of this sort should await appearance of a reasonably complete set of ab initio quantum mechanical calculations for small sulfur clusters.¹⁸ In the long run it is desirable to have the model potential reproduce the known crystal structures for sulfur,⁹ though the van der Waals forces involved in these structures are quite weak and may thus be largely irrelevant for the chemical reactivity studied in this paper.

The available experimental measurements of liquid sulfur pair correlation functions^{24,25} are few in number and too imprecise to

allow instructive comparisons with molecular dynamics simulation results. We hope the present paper and its predecessor¹¹ will stimulate more experimental activity that takes advantage of recent advances in instrumentation.

While the perturbation proposal outlined in section VI looks promising, it needs to be supported by (a) more simulation studies of $g(r,\lambda)$ at λ values between 0 and 1, (b) development of analytical theory for $g(r,0)$ and for $f_0(T,\rho)$, and (c) examination of the way that decreasing λ below 1 affects the polymerization anomaly in the liquid, observed experimentally at 159 °C.¹⁰

Finally, we mention that the present class of interaction models could be used to investigate the possibility of divalent, but topologically distinctive, polymeric species. These include interlinked large rings (sulfur analogues of the catenanes) and knotted rings. Adroit selection of initial atom positions, followed by steepest descent motions on the potential energy hypersurface, should help to estimate the lower size limits for sulfur clusters which could exhibit such unusual structures without undue steric hindrance.

Registry No. S, 7704-34-9; S_8 , 10544-50-0.

(24) Tompon, C. W.; Gingrich, N. S. *J. Chem. Phys.* **1959**, *31*, 1598.

(25) Poltavtsev, Yu. G.; Titenko, Yu. V. *Russ. J. Phys. Chem. (Engl. Transl.)* **1975**, *49*, 178.